

## Heparan Sulfate Degradation: Relation to Tumor Invasive and Metastatic Properties of Mouse B16 Melanoma Sublines

**Abstract.** After transport in the blood and implantation in the microcirculation, metastatic tumor cells must invade the vascular endothelium and underlying basal lamina. Mouse B16 melanoma sublines were used to determine the relation between metastatic properties and the ability of the sublines to degrade enzymatically the sulfated glycosaminoglycans present in the extracellular matrix of cultured vascular endothelial cells. Highly invasive and metastatic B16 sublines degraded matrix glycosaminoglycans faster than did sublines of lower metastatic potential. The main products of this matrix degradation were heparan sulfate fragments. Intact B16 cells (or their cell-free homogenates) with a high potential for lung colonization degraded purified heparan sulfate from bovine lung at higher rates than did B16 cells with a poor potential for lung colonization. Analysis of the degradation fragments indicated that B16 cells have a heparan sulfate endoglycosidase. Thus the abilities of B16 melanoma cells to extravasate and successfully colonize the lung may be related to their capacities to degrade heparan sulfate in the walls of pulmonary blood vessels.

In blood-borne tumor metastasis, malignant cells are spread to distant, often specific, organ sites (1). After implantation in the microcirculation, metastatic tumor cells must cross both the endothelial cell layer and the underlying basement membrane or basal lamina (1). This process appears to be dependent, in part, on tumor cell enzymes capable of degrading extracellular components of host tissues (2-7). The interactions between malignant cells and vascular endothelium have been studied in monolayers of

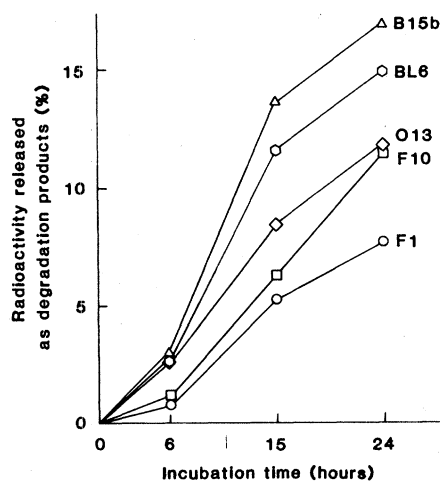


Fig. 1. Solubilization of sulfated glycosaminoglycans from subendothelial matrix by B16 melanoma metastatic variants. The degradation assay was performed as described (5, 6) except that  $3 \times 10^5$  B16 melanoma cells were plated on [ $^{35}\text{S}$ ]sulfate-labeled subendothelial matrix produced by bovine endothelial cells in culture (plate diameter, 35 mm). Radioactive counts resulting from a nonenzymatic process (5) were subtracted from the raw data. Each symbol represents the average of triplicate samples (standard deviation < 1 percent). The least significant difference and *Q* tests for significance of the means at  $P = .05$  or  $.01$  (20) at 24 hours show that F1 differs significantly from the other sublines and that F10 and O13 differ significantly from BL6 and B15b.

vascular endothelial cells that synthesize an extracellular matrix resembling the basal lamina (5-8). With this model, we found that metastatic tumor cells degrade matrix glycoproteins such as fibronectin and matrix-sulfated glycosaminoglycans such as heparan sulfate (5). Since heparan sulfate was released in solution as fragments approximately one-third their original size, we proposed that metastatic tumor cells have a heparan sulfate endoglycosidase (5). We have now examined a series of sublines of mouse melanoma cells of different metastatic potentials for their abilities to degrade sulfated proteoglycans of the subendothelial matrix as well as purified heparan sulfate from lung.

Malignant tumors are composed of heterogeneous mixtures of cells with widely different metastatic potentials (1). Procedures for selection in vivo have yielded B16 melanoma cells with increased potential for colonization of lung (9), brain (10), ovary (11), or liver (12), whereas techniques for selection in vitro have yielded B16 cells with increased invasiveness of tissues (13) or blood veins (14). We have used early passage sublines with low (B16-F1) or high (B16-F10) potential for lung colonization, high potential for colonization of ovary (B16-O13) or brain (B16-B15b), or a high potential for tissue invasion (B16-BL6) (15).

We had found earlier that B16-BL6 cells solubilized sulfated glycosaminoglycans in the subendothelial matrix at higher rates than did B16-F1 cells (6). We therefore examined the abilities of five B16 sublines to solubilize matrix labeled with [ $^{35}\text{S}$ ]sulfate and found that sublines with higher potentials for metastatic and organ colonization had significantly higher activities (Fig. 1).

We also examined five B16 sublines for their abilities to degrade purified lung

heparan sulfate in vitro and we analyzed the heparan sulfate fragments by polyacrylamide gel electrophoresis (16). With this technique, purified glycosaminoglycans, after being stained, show single, broad spots resulting from polymer heterogeneity. A plot of the logarithm of molecular weight of the glycosaminoglycans against their relative average migrations in the gel forms a straight line (Fig. 2A). The stained gels were scanned with a densitometer (Fig. 2B) and the relative heparan sulfate-degrading activity was determined by measuring the decrease in the first half of the densitometric peak (shaded areas in Fig. 2), which represents the higher molecular weight molecules of heparan sulfate. The pH optimum for degradation of heparan sulfate by B16 cell homogenates was approxi-

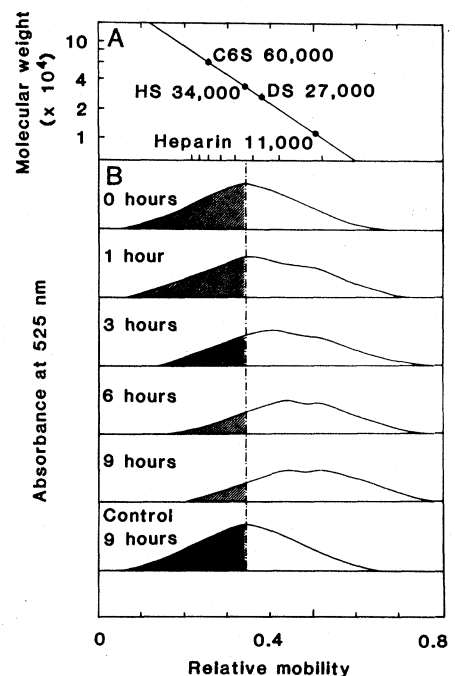


Fig. 2. Electrophoresis of lung heparan sulfate and its degradation products. Samples of purified heparan sulfate from bovine lung were incubated with homogenates prepared from B16-F10 melanoma cells for various times. A control sample contained a boiled cell homogenate. The samples were prepared for electrophoresis, and the gels were stained with toluidine blue and scanned with a densitometer (16). (A) Relative mobilities were determined and compared to the standard glycosaminoglycans chondroitin 6-sulfate (C6S) (molecular weights,  $\sim 60,000$  and  $\sim 40,000$ ), heparan sulfate (HS) (molecular weight,  $\sim 34,000$ ), dermatan sulfate (DS) (molecular weight,  $\sim 27,000$ ), chondroitin 4-sulfate (molecular weight,  $\sim 12,000$ ), and heparin (molecular weight,  $\sim 11,000$ ). (B) The decrease in total area of the densitometry peak indicates degradation of heparan sulfate to low molecular weight components not retained on the gel. The decrease in the left portion of the peak (shaded area) indicates degradation of high molecular weight heparan sulfate to intermediate and low molecular weight components.

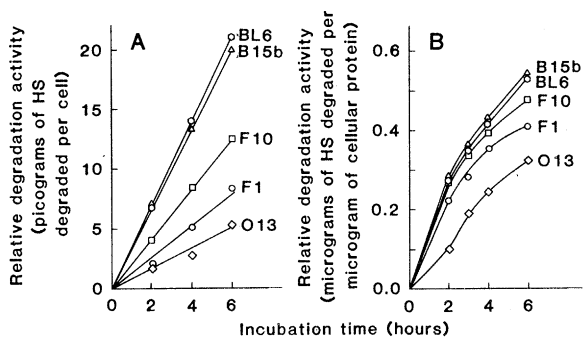


Fig. 3. Time course of degradation of lung heparan sulfate (HS) by intact, viable cells and cell-free homogenates of B16 melanoma metastatic variants. (A) Cells ( $1 \times 10^5$ ) were incubated with 50  $\mu$ g of purified heparan sulfate from bovine lung for various times in 200  $\mu$ l of medium (15) containing 20 mM Tricine (pH 7.3) at 37°C. (B) Cell homogenates were incubated with purified heparan sulfate [for assay conditions see Fig. 2 and (16)]. The relative degradation activities were calculated from the decrease in area of the high molecular weight half of the heparan sulfate peak (Fig. 2B). Each symbol represents the average of quadruplicate samples (standard deviation < 10 percent of data). The least significant difference and *Q* tests for significance of the means at *P* = .05 or .01 (20) at 6 hours show that F1 differs significantly from the other sublines and that F10 differs significantly from BL6 and B15b.

relative degradation activities were calculated from the decrease in area of the high molecular weight half of the heparan sulfate peak (Fig. 2B). Each symbol represents the average of quadruplicate samples (standard deviation < 10 percent of data). The least significant difference and *Q* tests for significance of the means at *P* = .05 or .01 (20) at 6 hours show that F1 differs significantly from the other sublines and that F10 differs significantly from BL6 and B15b.

mately 5, but we performed all assays at pH 6 to prevent precipitation of cell proteins. Of the five glycosaminoglycans used as substrates (heparan sulfate, heparin, chondroitin 6-sulfate, chondroitin 4-sulfate, and dermatan sulfate), lung heparan sulfate was degraded at higher rates by B16 cell homogenates than any other glycosaminoglycan tested, in agreement with our earlier observations that heparan sulfate is the predominant glycosaminoglycan solubilized from sub-endothelial matrix by B16 cells (5).

When heparan sulfate from bovine lung was incubated with B16 cells, the rates of appearance of degradation products of decreased molecular weights (Fig. 3) were higher than the rates of total degradation of heparan sulfate (data not shown), indicating that heparan sulfate of high molecular weight was degraded to large fragments rather than to monosaccharides. This suggests the action of an endoglycosidase capable of acting on heparan sulfate, a conclusion consistent with our previous results indicating that B16 melanoma cells degrade heparan sulfate from subendothelial matrix to discrete fragments (5). In addition, the same degradation products were obtained when B16 cell homogenates were incubated with lung heparan sulfate in the presence of D-saccharic acid 1,4-lactone (an inhibitor of  $\beta$ -glucuronidase). These products could be easily separated from undegraded heparan sulfate by gel chromatography on Sephadex G-75 or Sephacryl S-200 in pyridine-acetate buffer (data not shown).

When we compared the various B16 sublines for their activities in degrading lung heparan sulfate, using either intact cells (Fig. 3A) or their cell-free homogenates (Fig. 3B), we found that the sublines with the highest lung colonization potentials, such as B16-BL6 and B16-F10, had the highest degradation activities, and the sublines with the lowest

lung colonization potentials, such as B16-O13 and B16-F1, had the lowest activities. These differences were significant (see legend to Fig. 3). The decreases in degradation rates at the later incubation times (Fig. 3) probably represent substrate depletion, since the total amount of substrate added to the assay had to be limited in order to determine its quantity by the techniques we used (16). The fact that intact cells were able to degrade heparan sulfate suggested that specific endoglycosidases are present on the cell surface as membrane-bound enzymes, or they are released from cells. The heparan sulfate-degrading enzyme has been partially purified from B16 cells by affinity chromatography on columns of immobilized concanavalin A and therefore may be a glycoprotein. We have also found heparan sulfate endoglycosidase activities in homogenates of normal cells in which the enzyme concentrations appear to be related to the abilities of the cells to invade blood vessel walls. Thus, blood leukocytes had high concentrations of heparan sulfate endoglycosidase (relative activity per cellular protein), whereas fibroblasts had low concentrations.

Other enzymatic activities have been correlated with metastasis. Liotta *et al.* (4) found that the abilities to degrade type IV collagen, but not other types, were related to B16 metastatic potentials. Sloane *et al.* (3) reported that the amounts of the lysosomal cathepsin B in B16 cells correlate with metastatic potential. Cathepsin B can also degrade collagen and activate latent collagenases (17). We found that the activity of a specific glycosaminoglycan-degrading enzyme, heparan sulfate endoglycosidase, also correlates with the malignant behavior of B16 cells and their ability to colonize the lung. In our results, sublines B16-O13 and B16-F10 solubilized the sulfated glycosaminoglycans of the

extracellular matrix of endothelial cells at similar rates (Fig. 1). However, ovary-colonizing B16-O13 cells showed the lowest activity in degrading purified lung heparan sulfate (Fig. 3), suggesting that lung heparan sulfate degradation may require a specific endoglycosidase or that matrix degradation may require, in addition, proteolytic activities.

Heparan sulfate-degrading endoglycosidases have been described in various tissues (18), but their physiological function is still unknown. An endoglucuronidase in murine mastocytoma cells that specifically degrades macromolecular heparin to physiologically active fragments has been reported (19). Further studies should elucidate the role of this heparan sulfate endoglycosidase in tumor cell invasion and metastasis.

MOTOWO NAKAJIMA  
TATSURO IRIMURA

Department of Tumor Biology,  
University of Texas System Cancer  
Center, M. D. Anderson Hospital and  
Tumor Institute, Houston 77030

DANIELA DI FERRANTE\*  
NICOLA DI FERRANTE

Laboratories of Connective Tissue  
Research, Department of Biochemistry,  
Baylor College of Medicine,  
Houston, Texas 77030

GARTH L. NICOLSON  
Department of Tumor Biology,  
University of Texas System Cancer  
Center, M. D. Anderson Hospital  
and Tumor Institute

#### References and Notes

1. G. Poste and I. J. Fidler, *Nature (London)* **283**, 139 (1980); I. J. Fidler and G. L. Nicolson, *Cancer Biol. Rev.* **2**, 171 (1981); G. L. Nicolson, *Biochim. Biophys. Acta* **695**, 113 (1982); and G. Poste, *Curr. Probl. Cancer* **7** (No. 6), 1 (1982).
2. M. H. Dresden, S. A. Heilman, J. D. Schmidt, *Cancer Res.* **32**, 993 (1972); K. Hashimoto, Y. Yamanishi, E. Maeyens, M. K. Dabbous, T. Kanzaki, *ibid.* **33**, 2790 (1973); A. R. Poole, K. J. Tiltman, A. D. Recklies, T. A. M. Stoker, *Nature (London)* **273**, 545 (1978).
3. B. F. Sloane, J. R. Dunn, K. V. Honn, *Science* **212**, 1151 (1981); B. F. Sloane, K. V. Honn, J. G. Slader, W. A. Turner, J. J. Kimpson, J. D. Taylor, *Cancer Res.* **42**, 980 (1982).
4. L. A. Liotta, K. Tryggvason, S. Garbisa, I. R. Hart, C. M. Foltz, S. Shafiq, *Nature (London)* **284**, 67 (1980).
5. R. H. Kramer, K. G. Vogel, G. L. Nicolson, *J. Biol. Chem.* **257**, 2678 (1982).
6. G. L. Nicolson, *J. Histochem. Cytochem.* **30**, 214 (1982).
7. I. Vlodyavsky, Y. Ariav, R. Atzmon, Z. Fuks, *Exp. Cell Res.* **140**, 149 (1982).
8. R. H. Kramer and G. L. Nicolson, *Proc. Natl. Acad. Sci. U.S.A.* **76**, 5704 (1979).
9. I. J. Fidler, *Nature (London) New Biol.* **242**, 148 (1973).
10. K. W. Brunson, G. Beattie, G. L. Nicolson, *Nature (London)* **272**, 543 (1978); A. Raz and I. R. Hart, *Br. J. Cancer* **42**, 331 (1980); K. M. Miner, T. Kawaguchi, G. W. Uba, G. L. Nicolson, *Cancer Res.* **42**, 4631 (1982).
11. K. W. Brunson and G. L. Nicolson, *J. Supramol. Struct.* **11**, 517 (1979).
12. T-W Tao, A. Matter, K. Vogel, M. M. Burger, *Int. J. Cancer* **23**, 854 (1979).
13. I. R. Hart, *Am. J. Pathol.* **97**, 587 (1979).
14. G. Poste, J. Doll, I. R. Hart, I. J. Fidler, *Cancer Res.* **40**, 1636 (1980).
15. B16 melanoma sublines were grown to subcon-

fluence in a 1:1 mixture of Dulbecco-modified Eagle's and F12 medium supplemented with 5 percent heat-inactivated fetal bovine serum (Reheis Chemical Co.) and 1 percent nonessential amino acids without antibiotics. Cells were rinsed twice in medium without serum, detached in calcium- and magnesium-free phosphate-buffered saline containing 2 mM EDTA, and rinsed again in medium without serum before use. The cells were used within ten passages from frozen stocks and were found to be free from mycoplasma contamination [T. R. Chen, *Exp. Cell Res.* **104**, 255 (1977)].

16. J. C. Hilborn and P. A. Anastassiadis, *Anal. Biochem.* **39**, 88 (1971); C. P. Dietrich and H. B. Nader, *Biochim. Biophys. Acta* **343**, 34 (1974); C. P. Dietrich and S. M. C. Dietrich, *Anal. Biochem.* **70**, 645 (1976). Purified heparan sulfate from bovine lung (50  $\mu$ g) was incubated with each cell homogenate (40  $\mu$ g of protein) or a boiled cell homogenate in 70  $\mu$ l of 0.1M sodium phosphate, 0.2 percent Triton X-100, 0.15M sodium chloride, pH 6.0 at 37°C for various times. After incubation, the mixtures were centrifuged to remove debris and 2  $\mu$ l of the supernatants were applied to 6 percent polyacrylamide gels in 50 mM 1,3-diaminopropane acetate buffer, pH 9.0. Electrophoresis was per-

formed at 120 V for 60 minutes at 4°C. Electrophoresed gels were fixed and then stained with 0.1 percent toluidine blue in 1 percent acetic acid. Sulfated glycosaminoglycans larger than octasaccharides can be stained and scanned at 525 nm for quantification.

17. M. C. Burleigh, A. J. Barrett, G. S. Lazarus, *Biochem. J.* **137**, 387 (1974).  
 18. U. Klein, H. Kresse, K. von Figura, *Biochem. Biophys. Res. Commun.* **69**, 158 (1976); M. Höök, Å. Wasteson, A. Oldberg, *ibid.* **67**, 1422 (1975); Å. Wasteson, B. Glimelius, C. Bush, B. Westermark, C-H. Heldin, B. Norling, *Thromb. Res.* **11**, 309 (1977); U. Klein and K. von Figura, *Biochem. Biophys. Res. Commun.* **73**, 569 (1976).  
 19. S. Ögren and U. Lindahl, *J. Biol. Chem.* **250**, 2690 (1975).  
 20. G. W. Snedecor and W. G. Cochran, in *Statistical Methods*, (Iowa State University Press, Ames, ed. 6, 1967), p. 271.  
 21. We thank N. Wilson and S. Custead for their assistance. This work was supported by National Cancer Institute grants RO1-CA-28867 (G.L.N.) and RO1-AM-26482 (N.D.F.).  
 \* To whom correspondence should be addressed.

20 August 1982; revised 2 November 1982

## Radioactive Labeling of Antibody: A Simple and Efficient Method

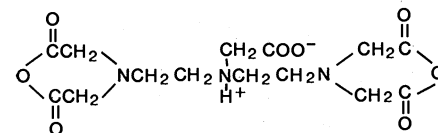
**Abstract.** A simple and efficient method of covalently coupling the strong chelator diethylenetriaminepentaacetic acid to proteins was developed for radiolabeling immunoglobulin G antibodies. After being coupled and labeled with indium-111, a monoclonal antibody to carcinoembryonic antigen retained its ability to bind to its antigen *in vitro* and *in vivo*. In nude mice with a human colorectal xenograft, 41 percent of the injected radioactivity became localized in each gram of xenograft at 24 hours compared with 9 percent for control antibody and 19 percent for radioiodinated antibody to carcinoembryonic antigen.

The detection of tumor tissue by radioimmunological methods is receiving considerable attention as a result of the development of hybridoma technology. One assessment is that the use of radiolabeled monoclonal antibody will obviate many of the problems that occur when affinity purified antibody is used for this purpose. A difficulty that will not be alleviated in this way is that of the radiolabel; most investigators continue to use  $^{131}\text{I}$  as the externally detectable tracer despite its poor imaging characteristics, somewhat involved labeling procedures, and high degree of instability on antibody *in vivo* (1). Alternative labeling methods have been investigated in which strong chelating groups are covalently attached to proteins so that they may be radiolabeled with metallic radionuclides, often resulting in high stability *in vivo*. Using a method developed by Krejcarek and Tucker (2), Khaw *et al.* (3) coupled diethylenetriaminepentaacetic acid (DTPA) to immunoglobulin G (IgG) fragments active against myosin and investigated the localization of the  $^{111}\text{In}$ -labeled protein in canine myocardial infarcts. Recently, Scheinberg *et al.* (4) used both this method and that of Yeh *et al.* (5) to prepare  $^{111}\text{In}$ -labeled monoclonal antibody specific for erythroleukemic cells

in mice. Although these and other methods provide coupled proteins, they are invariably characterized by complicated syntheses and, most important, by low coupling efficiencies. As a consequence

of coupling efficiencies of less than 1 percent, lengthy purification procedures are required to remove hydrolytic products.

We have developed a simple and efficient method of covalently coupling DTPA to proteins by using the bicyclic anhydride of DTPA. The anhydride is prepared by a one-step synthesis and, when protected from moisture, is stable for many months at room temperature. Characterization by infrared spectroscopy, nuclear magnetic resonance (6), and mass spectroscopy confirmed the structure of the anhydride to be:



Coupling to antibodies is accomplished as described previously for albumin and fibrinogen (6, 7). A solution of the antibody (typically 20  $\mu$ l containing 0.3 mg of protein) buffered at pH 7.0 with 0.05M bicarbonate is added to the solid anhydride (typically 0.7 to 0.9  $\mu$ g) and the solution is agitated for 1 minute. Coupling efficiency, defined as the percentage of anhydride molecules that covalently attach to the protein, is  $70 \pm 5$  percent when reacted at anhydride-to-protein molar ratios of 1:1 and, under these conditions, the IgG antibodies possess an average of 0.7 DTPA groups per molecule. The efficiency of coupling decreases at pH values above or below neutrality, with increasing anhydride-to-

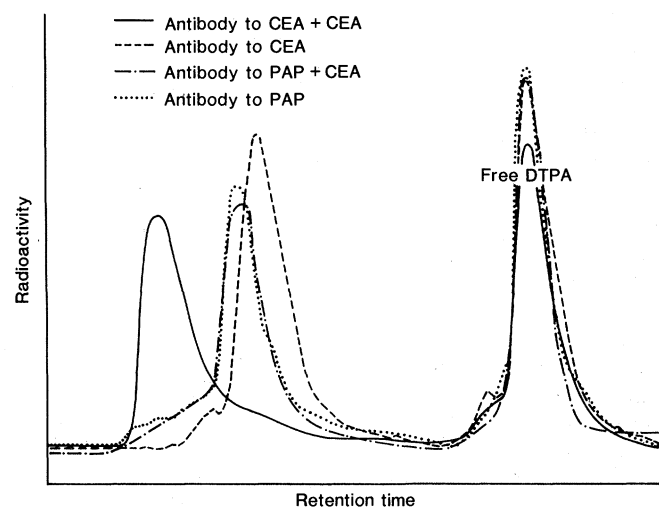


Fig. 1. Radioactivity traces obtained by HPLC analysis of  $^{111}\text{In}$ -labeled antibodies to CEA and PAP samples both with and without CEA. Samples with the antibody to CEA consisted of two identical solutions containing 22  $\mu$ g of labeled antibody (specific activity, 1.2  $\mu\text{Ci}/\mu\text{g}$ ) in 80  $\mu$ l of 2 percent bovine serum albumin, 0.05M HEPES buffer, and 0.9 percent NaCl. To one sample, 30  $\mu$ l of a solution of CEA (1  $\mu\text{g}/\mu\text{l}$ ) was added and the samples were

analyzed. The samples with antibody to PAP were prepared in the same way, except that only 13  $\mu$ g of labeled antibody was present (specific activity, 3.0  $\mu\text{Ci}/\mu\text{g}$ ). All four samples were unpurified from free DTPA so that the  $^{111}\text{In}$ -labeled free DTPA peak could serve as a marker. Since the molecular weights of CEA and IgG are roughly equal, a large shift to higher molecular weight and shorter retention times is expected in the case where binding with the antigen occurs. This shift to shorter retention time is apparent only in the radioactivity traces for the sample containing antibody to CEA. An identical shift was observed in the corresponding ultraviolet traces.